Nuclear Instruments and Methods in Physics Research A 360 (1995) 416–422

NUCLEAR INSTRUMENTS & METHODS IN PHYSICS RESEARCH Section A

ELSEVIER

Operational experience with the 4π ring imaging Cherenkov detector of DELPHI

W. Adam [d], E. Albrecht [d], D. Allen [d], M.-L. Andrieux [i], G. van Apeldoorn [o], Y. Arnoud [c], C. Aubret [b], A. Augustinus [o], P. Baillon [d], M. Battaglia [r], M. Berggren [q], D. Bloch [f], O. Botner [s], C. Bourdarios [j], J.M. Brunet [b], A.P. Budziak [k], A. Buys [d], P. Carecchio [i], P. Carrié [d], P. Cavalli [i], G. Gerutti [d], M. Chevry [m], E. Christophel [f], E. Dahl-Jensen [n], G. Damgaard [n], N. Dimitriou [g], B. D'Almagne [j], M. Davenport [d], J. Dolbeau [b], M. Dracos [f], M. Dris [p], L.-O. Eek [s], T. Ekelöf [s], J.P. Engel [f], D. Fassouliotis [p], T.A. Filippas [p], E. Fokitis [p], F. Fontanelli [h], A. Fontenille [i], D. Fraissard [d], F. Fulda [j], H. Fürstenau [d], J. Garcia [q], E.N. Gazis [p], D. Gillespie [d], V. Gracco [h], L. Guglielmi [b], F. Hahn [t], S. Haider [o], A. Hallgren [s], W. Hao [o], T. Henkes [d], P.F. Honoré [b], K. Huet [m], S. Ilie [d], P. Ioannou [a], P. Juillot [f], E. Karvelas [g], S. Katsanevas [a], E. Katsoufis [p], N. Kjaer [n], P.M. Kluit [o], B. Koene [o], C. Kourkoumelis [a], G. Lecoeur [d], G. Lenzen [t], L.-E. Lindqvist [s], A. López Agüera [q], D. Loukas [g], A. Maltezos [g], S. Maltezos [p], A. Markou [g], J. Medbo [s], J. Michalowski [k], F. Montano [h], G. Mourgue [d], B.S. Nielsen [n], R. Nicolaidou [a], J.M. Ostler [d], Th.D. Papadopoulou [p], A. Petrolini [h], G. Polok [k], D. Poutot [b], H. Rahmani [p], M. Reale [t], L.K. Resvanis [a], G. Sajot [i], M. Sannino [h], E. Saragas [g], E. Schyns [t,*], S. Squarcia [h], P. Stassi [i], R. Strub [f], J. Thadome [t], G.E. Theodosiou [g], D.Z. Toet [o], L. Traspedini [h], G. Tripodi [h], G. Tristram [b], A. Tsirou [d], O. Ullaland [d], A.S. de la Vega [e], M. Zavrtanik [l], E. Zevgolatakos [g]

[a] *University of Athens, Physics Department, Physics Laboratory, Solonos Str. 104, GR-10680 Athens, Greece*
[b] *Collège de France, Laboratoire de Physique Corpusculaire, 11 place Marcelin-Berthelot, F-75231 Paris, France*
[c] *CENS Centre d'Etudes Nucléaires de Saclay, DSM / DAPNIA / SPP, Service de Physique des Particules, F-91191 Gif-sur-Yvette Cedex, France*
[d] *CERN, CH-1211 Geneva 23, Switzerland*
[e] *COPPE / UFRJ, Dept. de Fisicà, Universidad Federal do Rio de Janeiro, Ilha do Fundão, 21945 Rio de Janeiro, Brazil*
[f] *CRN Centre de Recherches Nucléaires, B.P. 20 CRO, F-67037 Strasbourg Cédex, France*
[g] *Institute of Nuclear Physics, N.C.S.R. 'Demokritos', P.O. Box 60228, GR-15310 Aghia Paraskevi, Attiki, Greece*
[h] *Dipartimento di Fisica, Università di Genova and INFN, Via Dodecaneso 33, I-16146 Genova, Italy*
[i] *Institut des Sciences Nucléaires, Université de Grenoble 1, F-38026 Grenoble, France*
[j] *LAL Laboratoire de l'Accélérateur Linéaire, Université de Paris-Sud (Paris XI), Bâtiment 200, F-91405 Orsay Cédex, France*
[k] *High Energy Physics Laboratory, Inst. of Nucl. Physics, Ul. Kawiory 26a, PL-30055 Krakow 30, Poland*
[l] *Institut "Jozef Stefan", Ljubljana, Slovenia*
[m] *Université de Mons-Hainaut, Service de Physique des Particules Elémentaires, Faculté des Sciences, Av. Maistriau 15, B-7000 Mons, Belgium*
[n] *Niels Bohr Institute, Blegdamsvej 17, DK-2100 Copenhagen, Denmark*
[o] *NIKHEF-H, Postbus 41882, NL-1009 DB Amsterdam, The Netherlands*
[p] *NTU National Technical University, Physics Laboratory II, 9 Heroes of Polytechneion Street, Zografou, GR-15780 Athens, Greece*
[q] *Facultad de Ciencias, Universidad de Santander, av. de los Castros, E-39005 Santander, Spain*

[*] Corresponding author.

SSDI 0168-9002(94)01624-0

[r] Research Institute for High Energy Physics, SEFT, Siltavuorenpenger 20c, SF-00170 Helsinki, Finland
[s] Dept. of Radiation Sciences, University of Uppsala, P.O. Box 535, S-751 21 Uppsala, Sweden
[t] Fachbereich Physik, University of Wuppertal, Gauss-Str. 20, D-42097 Wuppertal, Germany

Abstract

The ring imaging Cherenkov detector in the DELPHI Experiment at LEP allows hadron identification over a momentum range up to about 40 Gev/c over a near to 4π solid angle. Photons emitted by charged particles traversing gas and liquid radiators which are filled with UV-transparent perfluorocarbons, are used for Cherenkov angle reconstruction. Stable operation ensures that the detector is an efficient and powerful instrument. Monitoring of the detector parameters is of utmost importance to achieve good data quality and adequate data processing. The hadron identifying power of the ring imaging Cherenkov detector closely meets the main design values. Computerized control and monitoring features of the different subsystems will be presented. The interplay between detector parameters and the particle separating capacity of the detector will be discussed.

1. Introduction

The DELPHI experiment (DEtector with Lepton, Photon and Hadron Identification) [1] at the Large Electron–Positron collider at CERN is equipped with Ring Imaging Cherenkov (RICH) detectors. Almost covering the full solid angle, the RICH detectors enable identification of pions, kaons and protons over most of the momentum range below 40 GeV/c.

Charged particles exceeding the velocity of light in a radiator medium emit Cherenkov radiation. Applying the equation $\beta = 1/(n \cos \theta_{\check{c}})$ gives:

$$m = p\sqrt{(n \cos \theta_{\check{c}})^2 - 1}\,, \qquad (1)$$

where $\beta = v/c$, n is the refractive index of the radiator medium, m is the particle mass, p is the particle momentum and $\theta_{\check{c}}$ is the emission angle of Cherenkov photons with respect to the particle track. The number of emitted photons per unit of length in the radiator is proportional to $1/\lambda$, where λ is the wavelength.

The DELPHI RICH detectors contain two systems of different geometry, as is shown in Fig. 1. The Forward RICH [2] in the two endcaps covers an active area of ~ 8 m^2 between the polar angles $15° < \theta < 35°$ and $145° < \theta < 165°$. The Barrel Rich [3] covers a cylindrical area of ~ 30 m^2 in the barrel region between the polar angles $40° < \theta < 140°$.

Forward and Barrel RICH are based on the same technique. They combine liquid and gaseous radiators with one photon detector. Cherenkov photons generate a conic section of photoelectrons in the photon detector. The photon detector consists of photosensitive time projection chambers which enable three dimensional reconstruction of the conversion point of each detected photon. The conversion points are then used together with particle tracking parameters to compute the Cherenkov angle $\theta_{\check{c}}$.

The DELPHI RICH is not a stand-alone system for particle identification. To ensure good information on the tracking parameters and the particle momentum p, the RICH is sandwiched between different tracking detectors inside the 1.2 T magnetic field (Fig. 1). The combined information of these tracking detectors gives a momentum resolution smaller than 5% for most particles.

The particle identifying power of the RICH depends on various detector parameters which have an influence on the resolution $\sigma_{\theta_{\check{c}}}$ of the Cherenkov angle measurement. Therefore stable operation of the different subsystems and monitoring of the relevant detector parameters is very important. All control and monitoring information is put on the DELPHI database and integrated with the physics data during the data processings. After background reduction, noise reduction and alignment, the Cherenkov angle is calculated for each track. The particle momentum, the background, the observed number of individual photoelectrons and their Cherenkov angle distribution are used to determine the likelihood for the particle being a pion, kaon or proton.

2. General operation

2.1. Photon production

The choice of the radiator medium consequently determines the momentum range where particle identification will be possible (Eq. (1)). To cover a wide momentum range the DELPHI RICH has combined liquid and gaseous radiator media for photon production. A total of 120 liquid radiators are filled with perfluorohexane (C_6F_{14}). The liquid radiators are 1 cm thick and have quartz windows facing the photon detector at a distance of ~ 115 mm and ~ 180 mm in the Barrel and the Forward RICH respectively. The 24 m^3 Barrel RICH gas radiator contains perfluoropentane (C_5F_{12}) whilst the 8 m^3 gas radiator of the Forward RICH is filled with perfluorobutane (C_4F_{10}).

Perfluorocarbons have been chosen mainly because they combine a suitable refractive index with good UV transmission and a low chromatic dispersion [4]. The most relevant properties of these fluids are listed in Table 1.

Cherenkov photons originating from the liquid radiator

directly enter the photon detector while photons from the gas radiator are reflected onto the photon detector by focusing mirrors, 408 in total. Their reflectivity is about 90% for wavelengths larger than 170 nm.

2.2. Cherenkov photon detection

In the Barrel and Forward RICH the photon detectors are arranged in 12 sectors in azimuth on each side of the

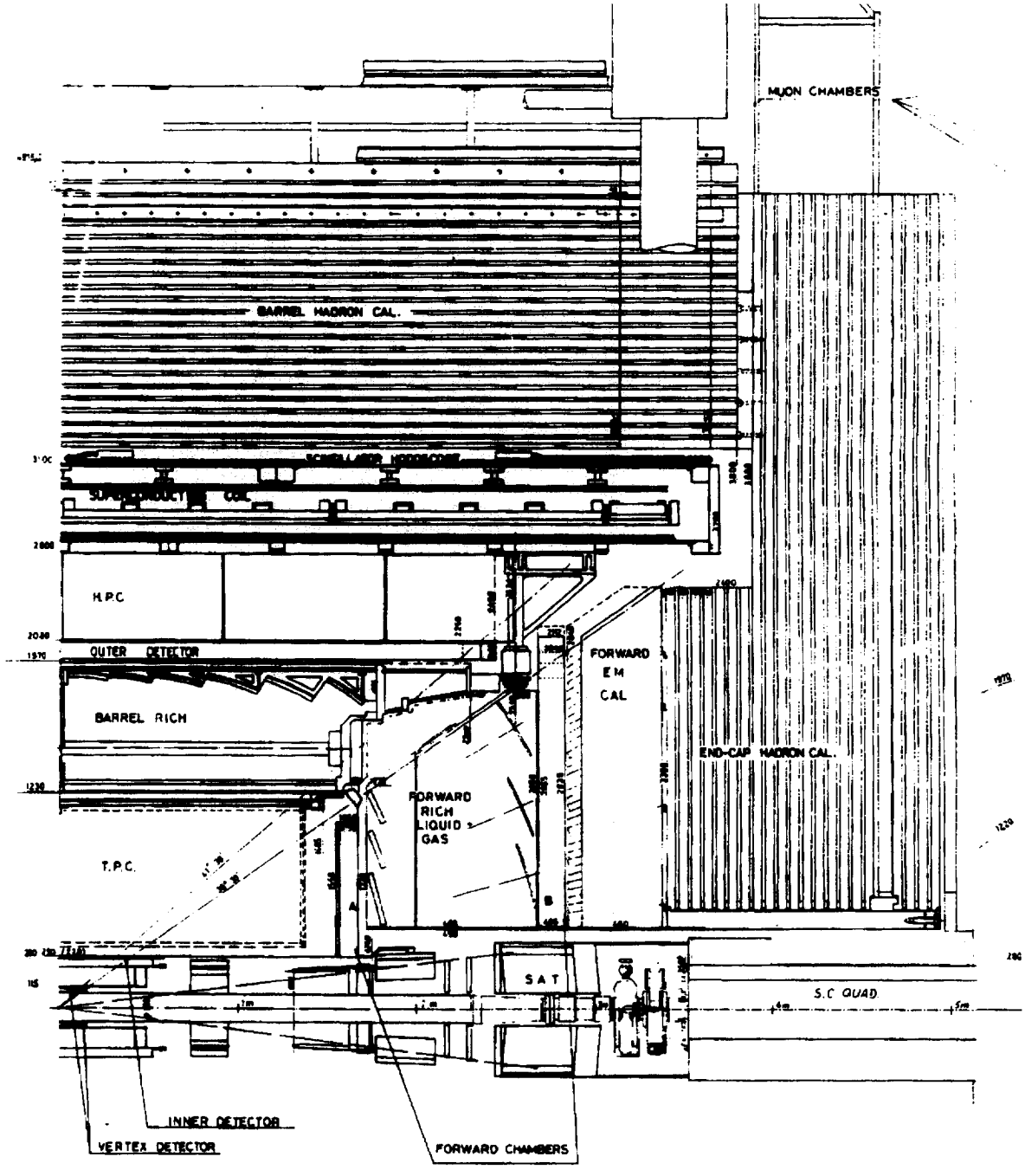

Fig. 1. Cross section along the beampipe of a quarter of the DELPHI detector. The Forward and Barrel RICH are sandwiched between the different tracking detectors: Time Projection Chamber (TPC), Outer Detector (OD), Forward Chambers A and B (FCA, FCB).

Table 1
Properties of C_4F_{10}, C_5F_{12} and C_6F_{14}

	C_4F_{10}	C_5F_{12}	C_6F_{14}
Boiling point (°C)	−2	28	57
Refractive index (at 7 eV)	1.00155	1.00172	1.283
Threshold for kaon (GeV/c)	9.0	8.3	0.62
UV transmission (1 atm.)	15 cm layer	15 cm layer	1 cm layer
162 nm	1.0	0.0	0.0
165 nm	1.0	0.58	0.0
170 nm	1.0	0.80	0.15
180 nm	1.0	0.96	0.80

barrel and in each endcap. Every sector is made of two quartz boxes containing a drift gas with an admixture of the photo-ionizing vapour tetrakis-dimethyl-amino-ethylene (TMAE) [5]. The ionization potential of TMAE is ~ 5.5 eV (~ 225 nm). The concentration of the TMAE is equivalent to its saturated vapour pressure at 28°C in the Barrel and 24°C in the Forward RICH. The Cherenkov photon mean free path is therefore ~ 24 mm in the Forward and ~ 18 mm in the Barrel RICH. Having a 50 mm average depth of the photon detector, this allows good discrimination between photoelectrons emitted by the gas and liquid radiators which are placed on opposite sides of the photon detector. Hence to avoid a miss-association for the Cherenkov angle reconstruction. The ringlike image of photoelectrons drifts towards one end of the quartz box where they are detected by multiwire proportional chambers (MWPCs). In the Barrel RICH the magnetic field of DELPHI is parallel to the electric drift field which ensures that small drift field inhomogeneities will hardly affect the photoelectron drift trajectories. The fields are orthogonal in the Forward RICH, causing the photoelectrons to drift under a Lorentz angle of ~ 50°.

Three-dimensional reconstruction of each photon conversion point is possible by drift time measurement combined with anode wire and cathode strip readout of the MWPC. The gas amplification is about 2×10^5 which gives a single photoelectron detection efficiency of ~ 90%. Blinds are placed between the anode wires for shielding against secondary photons originating from the avalanche process. The traversing particle itself produces a few hundred ionization electrons. This causes some crosstalk and a ~ 250 ns dead time in the readout system. Altogether the RICH has 39 168 MWPC readout channels.

To verify the electron drift velocity, all photon detectors are equipped with a calibration system [6]. This is a well defined geometrical formation of optical quartz fibres mounted on top of the mirror side of each photon detector box. UV light is sent into the photon detectors from a central lamp.

The RICH photon detection range is for photon wavelengths of 160 nm up to 220 nm. This is determined by the quartz UV transmission and the TMAE quantum efficiency. The quartz transmission goes from ~ 2% at 160 nm to ~ 90% at 220 nm setting the lower photon detection limit. The TMAE quantum efficiency ranges from ~ 40% at 160 nm to ~ 1% at 220 nm fixing the upper photon detection limit.

2.3. *The fluid systems*

The RICH radiator systems are recirculating systems whereas the photon detector gases are vented. Since water and oxygen are strong UV absorbers it is very important to remove them from the fluids to optimize the photoelectron yield. Water and oxygen filters are therefore included in the systems.

The Barrel RICH gas radiator is operated at a pressure of 1030 mbar. The pressure control of both the photon detector and liquid radiator systems must follow this pressure since they have fragile quartz components. The three fluid systems of the Barrel RICH are linked to rupture discs to safeguard them against too large differential pressure changes. Using C_5F_{12} as radiator gas requires the Barrel RICH to be heated to 40°C (Table 1). This allows a high TMAE saturated vapour temperature of 28°C in the drift gas which is a mixture of 75/25% methane/ethane.

The three Forward RICH fluid systems are operated at atmospheric pressure. With the use of C_4F_{10} the Forward RICH can be kept at the ambient temperature of the DELPHI detector (~ 32°C). The drift gas is pure ethane. The saturated TMAE vapour temperature is 24°C.

3. Monitoring and control

To achieve good data quality and adequate data processings, stable operation of the different subsystems and monitoring of the relevant detector parameters is very important. Safety and stability during data taking is maintained by computerized control and monitoring features of the numerous RICH subsystems. Rapid feedback is achieved by having the control systems interlinked via a vast computer network which also gives access to the DELPHI database.

On the Barrel RICH an extended computerized heating system uses about 400 sensors to monitor the temperature and to control the 40°C temperature within fluctuations of 0.3°C. No heating control is needed on the Forward RICH since it is operated at the ambient DELPHI temperature. However the temperature is monitored and stored on database. Special heating control maintains the constant TMAE temperature within ±0.1°C.

Sample lines from the gas radiator systems are connected to sonar-based devices which monitor the sound velocity in the radiator gases. A change in the composition of the gases will give a change in the sound velocity measurement [4].

The very high voltage for the drift field of the photon detectors and the high voltages of the MWPCs are con-

stantly monitored. Occasionally a MWPC might draw too high a current and will trip. The MWPC is ramped up to operational voltages again and the incident is recorded on the database.

An elaborate system controls and monitors the driftgas of the photon detectors. Before the drift gases are saturated with TMAE, oxygen and water are removed. Water is a very strong UV absorber and is monitored to be lower than 5 ppm. Oxidized TMAE products are very electronegative and will cause severe losses of photoelectrons. The oxygen content of the drift gas is kept well below 1 ppm.

The UV calibration system monitors the single photoelectron drift velocity. The maximum drift distance is 150 cm in the Barrel and 45 cm in the Forward RICH. On the Barrel RICH the system is operated at a rate of about 0.3 Hz. The Barrel RICH drift velocity is determined with an accuracy of 0.05%. It is therefore possible to observe slight fluctuations of $\sim 0.06\%$ in the drift velocity due to variations of ~ 1.5 mbar in the Barrel RICH pressure control. On the Forward RICH UV calibration is done before or after a physics run. Lorentz angle and drift velocity are parametrized as a function of pressure and temperature. In this way a precision in the drift velocity of $\sim 0.1\%$ is achieved.

Later this year, a Fabry–Perot interferometer will be installed to perform online measurements of the refractive indices of the different radiator fluids.

Monitoring on the electronics readout chain is performed by online data quality check facilities.

3.1. UV transmission and photon conversion depth

The UV transmission of the different perfluorocarbons is frequently monitored by online monochromator systems. UV light from a deuterium lamp is selected by a monochromator and sent into sample cells of variable depth via a beam splitter. The sample cells have quartz windows. The transmission is measured for liquid samples of 1 cm thickness at 25°C and for gas samples of 15 cm at 40°C. All measurements are done at atmospheric pressure. Multiple sample lines enable simultaneous measurement of gas and liquid over the photon detection range from 160 nm to 220 nm. The integrated transmission over this wavelength range may be taken as a measure of quality for the RICH radiator fluids. Expressing the range of acceptance in units of wavelength, an integral larger than 400 Å is considered a good value for C_6F_{14} liquids. For C_4F_{10} and C_5F_{12} gases, values larger than 520 Å are taken to be good.

The integral over the transmission folded with the TMAE quantum efficiency (Q_{eff}) gives an indication of the photoelectron yield in the photon detector. Therefore, with a larger integral one expects more detected photoelectrons and thus a smaller Cherenkov angle resolution leading to a better particle separation.

As an example, Fig. 2 shows monochromator measurements of the Forward RICH C_4F_{10} gas just before the start of 1994 running and during normal physics operation. From the latter one can see that the UV transmission is limited by the quartz cutoff at 1600 Å. Comparing the two measurements, there is a clear decrease in transmission in the region up to 1800 Å in the first curve, which would give a 43% reduction in the photoelectron yield, since photons traverse on average 60 cm of radiator gas before reaching the photon detector. This transmission dip was mainly due to UV absorption by water with an estimated concentration of 450 ppm. After recirculation through filters the transmission improves significantly up to the

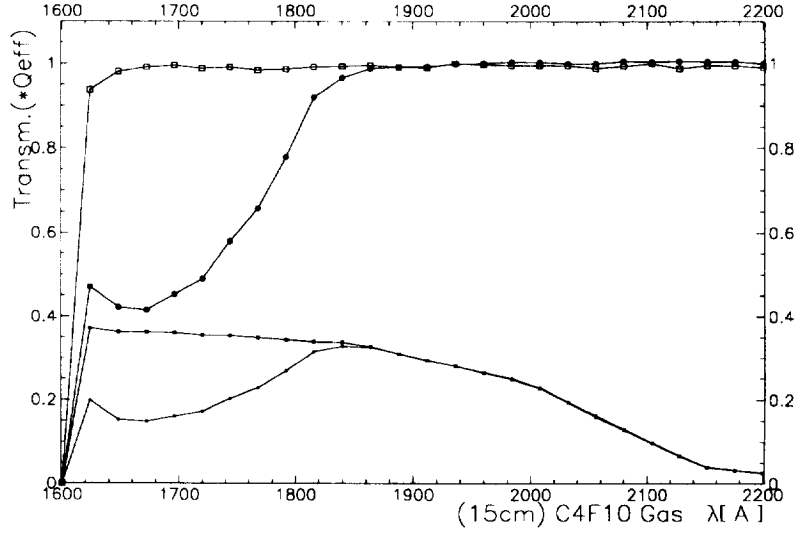

Fig. 2. UV transmission vs wavelength (in Å) of the Forward RICH C_4F_{10} gas radiator. ● = before start of 1994 physics, running, $\int_{1600}^{2200}(\text{Tr} \times Q_{\text{eff}}) = 117$ Å. □ = during normal operation, $\int_{1600}^{2200}(\text{Tr} \times Q_{\text{eff}}) = 148$ Å. The difference in transmission can be explained by a 450 ppm water contamination.

Table 2
The Cherenkov angle resolution for single photoelectrons from 1993 $Z^0 \to \mu^+\mu^-$ selected events

DELPHI RICH 1993	Forward RICH		Barrel RICH	
	Gas	Liquid	Gas	Liquid
σ_{θ_c} per p.e. (mrad)	2.0 ± 0.1	10.5 ± 0.2	4.2 ± 0.1	14.0 ± 0.2

value of normal running. Hence the monochromator systems also are a useful tool to monitor the cleaning efficiency of filters. The integrated transmission is very stable in time as is the average number of measured photoelectrons per track [7].

The monochromator systems also allow the monitoring of the photon conversion depth in the TMAE loaded gas. Fig. 3 shows the photon conversion depth versus wavelength for the Barrel RICH 28°C saturated vapour in the methane–ethane gas mixture. From this monochromator measurement the average photon conversion depth over the RICH photon detection range from 160 nm to 220 nm is 19.7 mm, not taking into account that Cherenkov photon production is proportional to $1/\lambda$. The average Cherenkov photon wavelength in the RICH is ~ 190 nm.

4. Processing and data quality

The monitoring and control information is read from the database during data processing. The database also contains the overall detector geometry as well as fixed detector survey information such as mirror reflectivities and quartz UV transmission. Very clean muon tracks arizing from $Z^0 \to \mu^+\mu^-$ are used for alignment purposes. There 45 GeV/c tracks give a maximum Cherenkov angle in both the RICH gas and liquid radiators. The RICH alignment process [8] performs a series of iterations in which the Cherenkov angle resolution is improved by slightly shifting or rotating the nominal positions of individual components of the detector. After each iteration the Cherenkov angle resolution is recalculated. Depending on the number of parameters up to a few hundred iterations can be needed to minimize the resolution. For the 1993 DELPHI two prong muon events the mean Cherenkov angle resolutions for the gas and liquid radiators are given in Table 2. These results closely correspond to the predictions given by simulations.

To verify whether one has good control over the detector parameters and systematic errors one can look at the mean resolution as a function of the number of photoelec-

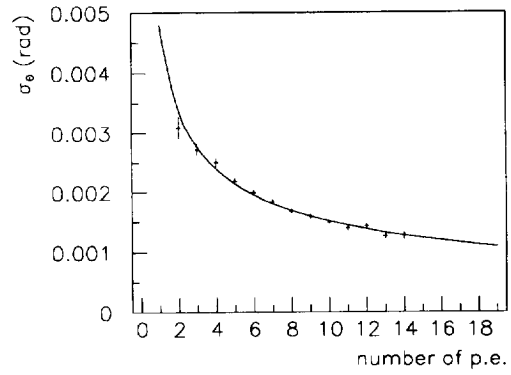

Fig. 4. The mean Cherenkov angle resolution for the Barrel RICH gas radiator vs the number of detected photoelectrons per ring from 1993 $Z^0 \to \mu^+\mu^-$ selected events.

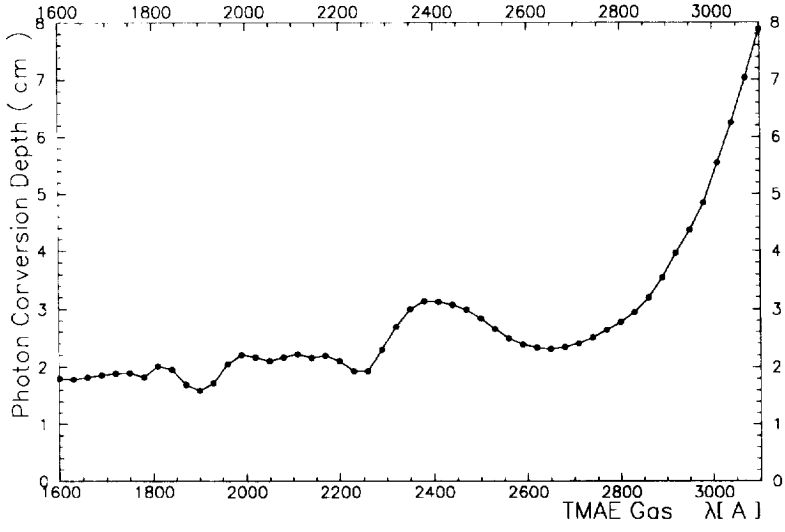

Fig. 3. Photon conversion depth vs wavelength of the Barrel RICH photon detector. The TMAE saturated vapour temperature is 28°C in 75/25% CH_4/C_2H_6 drift gas mixture.

trons per ring, N_{pe}. If the data quality is good and the systematic errors are small compared to the statistical errors, the Cherenkov angle resolution is expected to decrease proportional to $1/\sqrt{N_{pe}}$. This is illustrated in Fig. 4 for the Barrel RICH gas radiator.

With the newly aligned RICH geometry the hadronic events are processed and the Cherenkov angles for the tracks which passed through the RICH are reconstructed [9]. A probability of being a pion, kaon or proton is assigned to each particle.

5. Conclusions

The computerized control systems and the monitoring features of the DELPHI RICH have proven to be indispensable for safe and stable operation of the detector. The detector fluids are of good purity giving a satisfying production and detection of Cherenkov photons. The yield of suitable physics data is secured by accurate monitoring of the detector parameters. The results of the DELPHI RICH closely agree with the predictions of simulations. The RICH technique provides a strong support for the many DELPHI physics analyses which are based on particle identification.

Acknowledgements

Many physicists, engineers and technicians at the home institutes and at CERN have done invaluable work in preparing the RICH to reach the operational status in which it is now. We express our deep gratitude and appreciation to each of them for their competent work. We also thank the funding agencies for the continuous support of the project.

References

[1] P. Aarnio et al. (DELPHI Collaboration), Nucl. Instr. and Meth. A 303 (1991) 233.
[2] W. Adam et al., Nucl. Instr. and Meth. A 338 (1994) 284 and references therein.
[3] E.G. Anassontzis et al., Nucl. Instr. and Meth. A 323 (1992) 351 and references therein.
[4] G. Lenzen et al., Nucl Instr. and Meth. A 343 (1994) 268.
[5] R.A. Holroyd et al., Nucl. Instr. and Meth. A 261 (1987) 440.
[6] P. Adrianos et al., Nucl. Instr. and Meth. A 294 (1990) 424; A. Markou et al., DELPHI 91-95 RICH 45 (1991).
[7] G. van Apeldoorn et al., DELPHI 94-18 RICH 61, submitted to IEEE Trans. Nucl. Sci.
[8] M. Berggren, DELPHI 89-81 PROG 146.
[9] W. Adam et al., DELPHI 94-112 PHYS429, submitted to ICHEP94, GLS0188.